Critical phenomena of strange hadronic matter in the extended Zimanyi-Moszkowski model

K. Miyazaki*

Abstract

We have studied the liquid-gas phase transition of warm strange hadronic matter (SHM) in the extended Zimanyi-Moszkowski model. We implement the Nijmegen soft-core potential model NSC97f of hyperon-hyperon interactions in terms of the (hidden) strange mesons. The saturation properties of pure Λ and Ξ matter by the potential essentially determine the dependence of the critical temperature on the strangeness fraction of SHM. We treat the liquid-gas phase transition of SHM as the first-order one and employ Maxwell construction so as to calculate the phase coexistence curves. The derived critical exponents $\beta \simeq 1/3$ and $\gamma = 1.22$ are almost independent of the strangeness fraction of SHM and almost agree with the empirical values derived from the recent multifragmentation reactions. Consequently, we have confirmed the universality of the critical phenomena in the liquid-gas phase transition of hadronic system.

1 Introduction

Recently, there are renewed interests [1,2] on the liquid-gas phase transition in nuclear medium. The evidences of the first-order phase transition have been observed in the plateau of the caloric curves [3] and the negative heat capacity [4] from nuclear multifragmentation reactions. Moreover, we have the information on the critical phenomena of the phase transition, the critical temperature T_C [5-7] and the critical exponents β and γ [6,8-10]. It is generally believed that the critical phenomena are universal. We can expect that the critical exponents are independent of the kinds of matter. In fact, their values for nuclear matter derived from multifragmentation reactions [10] agree with their universal values in molecular physics. This is the most prominent evidence of nuclear liquid-gas phase transitions, and so is really surprising because the energy and length scales and the underlying fundamental interaction in nuclear physics are essentially different from those in molecular physics.

It is however noted [11] that in heavy-ion reactions the limit of Coulomb instability prevents the nuclear system from reaching the critical point. Therefore, the empirical

*E-mail : miyazakiro@rio.odn.ne.jp

values of the exponents are derived in the far region from the critical point [10], where we can expect that the mean-field theory of nuclear medium is still valid. In the recent works [12,13] the author has shown that the extended Zimanyi-Moszkowski (EZM) model [14,15] of relativistic mean-field theory [16] for nuclear matter can reproduce the empirical values of the critical exponents. It has been also found that they do not depend on the isospin asymmetry of nuclear matter.

It is a natural next step to extend the investigations of Refs. [12,13] to the liquid-gas phase transition in strange hadronic matter (SHM) [17-19]. Are the critical phenomena independent of the strangeness? It is the purpose of the present work to answer the question. In the next section we will develop the EZM model to describe warm SHM. In section 3 we perform numerical analyses of the critical phenomena in the liquid-gas phase transition of SHM with several strangeness fractions. In section 4 our investigations are summarized.

2 The EZM model

The EZM model for cold SHM taking into account the (hidden) strange mesons σ^* and ϕ [20] has already been developed in Ref. [21]. In the present work, we will extend it to finite temperature. The thermodynamic potential per volume $\tilde{\Omega} \equiv \Omega/V$ of SHM at temperature T is

$$\begin{aligned}\tilde{\Omega} &= \frac{1}{2} m_\sigma^2 \langle\sigma\rangle^2 + \frac{1}{2} m_{\sigma^*}^2 \langle\sigma^*\rangle^2 - \frac{1}{2} m_\omega^2 \langle\omega_0\rangle^2 - \frac{1}{2} m_\phi^2 \langle\phi_0\rangle^2 \\ &- T \sum_{\substack{B=N,\Lambda, \\ \Sigma,\Xi}} \gamma_B \int_0^\infty \frac{d^3\mathbf{k}}{(2\pi)^3} \left\{ \ln\left[1+\exp\left(\frac{\nu_B - E_{kB}^*}{T}\right)\right] + \ln\left[1+\exp\left(\frac{-\nu_B - E_{kB}^*}{T}\right)\right]\right\},\end{aligned} \tag{1}$$

where $M_B^* = m_B^* M_B$ and $E_{kB}^* = (\mathbf{k}^2 + M_B^{*2})^{1/2}$ are the effective mass and energy of each baryon in the SHM. In this work we set the Boltzmann constant as a unit. The spin-isospin degeneracy factor is defined as $\gamma_B = \{4, 2, 6, 4\}$ for $B = \{N, \Lambda, \Sigma, \Xi\}$. The ν_B is given by the chemical potential μ_B and the vector potential V_{0B} of each baryon as

$$\nu_B = \mu_B - V_{0B}. \tag{2}$$

The scalar mean-fields are determined [21] from the effective masses of N and Λ:

$$\bar{\sigma}_N = \frac{1 - m_N^*}{(1-\lambda_N) + \lambda_N m_N^*}, \tag{3}$$

$$\bar{\sigma}_\Lambda^* = \frac{2(1-m_\Lambda^*) - \left[2 - \frac{1}{2}(1-m_\Lambda^*)\right]\bar{\sigma}_\Lambda}{2 - \frac{1}{2}(2+m_\Lambda^*)\bar{\sigma}_\Lambda}, \tag{4}$$

where $\lambda_N = 1/3$ and we have introduced the reduced scalar mean-fields for each baryon,

$$\bar{\sigma}_B \equiv \frac{g_{BB\sigma}}{M_B} \langle \sigma \rangle \,, \tag{5}$$

$$\bar{\sigma}^*_Y \equiv \frac{g_{YY\sigma^*}}{M_Y} \langle \sigma^* \rangle \,. \tag{6}$$

The effective masses of Σ and Ξ are determined [21] by m^*_N and m^*_Λ through

$$m^*_\Sigma = \frac{2 - \frac{3}{2}\,\bar{\sigma}_\Sigma - 2\,\bar{\sigma}^*_\Sigma + \bar{\sigma}_\Sigma \bar{\sigma}^*_\Sigma}{D_\Sigma}, \tag{7}$$

$$m^*_\Xi = \frac{2 - 2\,\bar{\sigma}_\Xi - \frac{3}{2}\,\bar{\sigma}^*_\Xi + \bar{\sigma}_\Xi \bar{\sigma}^*_\Xi}{D_\Xi}, \tag{8}$$

where

$$D_{\Lambda(\Sigma)} = 2 + \frac{1}{2}\left(1 - \bar{\sigma}^*_{\Lambda(\Sigma)}\right) \bar{\sigma}_{\Lambda(\Sigma)}, \tag{9}$$

$$D_\Xi = 2 + \frac{1}{2}\left(1 - \bar{\sigma}_\Xi\right) \bar{\sigma}^*_\Xi. \tag{10}$$

The vector mean-fields are determined from the vector potentials of N and Λ:

$$\langle\, \omega_0 \rangle = \frac{V_{0N}}{g^*_{NN\omega}}, \tag{11}$$

$$\langle \phi_0 \rangle = \frac{V_{0\Lambda} - C^\Lambda_\omega V_{0N}}{g^*_{\Lambda\Lambda\phi}}, \tag{12}$$

where

$$C^\Lambda_\omega = \frac{g^*_{\Lambda\Lambda\omega}}{g^*_{NN\omega}}. \tag{13}$$

The vector potentials of Σ and Ξ are given by V_{0N} and $V_{0\Lambda}$ as

$$V_{0Y} = \left(\frac{g^*_{YY\omega}}{g^*_{NN\omega}} - \frac{g^*_{YY\phi}}{g^*_{\Lambda\Lambda\phi}} \frac{g^*_{\Lambda\Lambda\omega}}{g^*_{NN\omega}} \right) V_{0N} + \frac{g^*_{YY\phi}}{g^*_{\Lambda\Lambda\phi}}\, V_{0\Lambda}. \tag{14}$$

The effective vector-meson coupling constants $g^*_{BB\omega}$ and $g^*_{YY\phi}$ in Eqs. (11)-(14) are also determined [21] by m^*_N and m^*_Λ through

$$g^*_{NN\omega} = \left[(1 - \lambda_N) + \lambda_N m^*_N \right] g_{NN\omega}, \tag{15}$$

$$g^*_{\Lambda\Lambda(\Sigma\Sigma)\omega} = \frac{2 - \bar{\sigma}^*_{\Lambda(\Sigma)}}{D_{\Lambda(\Sigma)}}\, g_{\Lambda\Lambda(\Sigma\Sigma)\omega}, \tag{16}$$

$$g^*_{\Xi\Xi\omega} = \frac{2 - \frac{1}{2}\,\bar{\sigma}^*_\Xi}{D_\Xi}\, g_{\Xi\Xi\omega}, \tag{17}$$

$$g^*_{\Lambda\Lambda(\Sigma\Sigma)\phi} = \frac{2 - \frac{1}{2}\,\bar{\sigma}_{\Lambda(\Sigma)}}{D_{\Lambda(\Sigma)}}\, g_{\Lambda\Lambda(\Sigma\Sigma)\phi}, \tag{18}$$

$$g^*_{\Xi\Xi\phi} = \frac{2 - \bar{\sigma}_{\Xi}}{D_{\Xi}}\, g_{\Xi\Xi\phi}. \tag{19}$$

Finally, the effective masses m^*_N and m^*_Λ and the vector potentials V_{0N} and $V_{0\Lambda}$ are determined from extremizing the thermodynamic potential $\tilde{\Omega}$ by them. The results are

$$\rho_{bN} + \sum_{Y=\Sigma,\Xi}\left(\frac{g^*_{YY\omega}}{g^*_{NN\omega}} - \frac{g^*_{YY\phi}}{g^*_{\Lambda\Lambda\phi}}\frac{g^*_{\Lambda\Lambda\omega}}{g^*_{NN\omega}}\right)\rho_{bY} - \left(\frac{m_\omega}{g^*_{NN\omega}}\right)^2 V_{0N} + \left(\frac{m_\phi}{g^*_{\Lambda\Lambda\phi}}\right)^2 \left(V_{0\Lambda} - C^\Lambda_\omega V_{0N}\right) C^\Lambda_\omega = 0, \tag{20}$$

$$\rho_{b\Lambda} + \sum_{Y=\Sigma,\Xi}\frac{g^*_{YY\phi}}{g^*_{\Lambda\Lambda\phi}}\rho_{bY} - \left(\frac{m_\phi}{g^*_{\Lambda\Lambda\phi}}\right)^2 \left(V_{0\Lambda} - C^\Lambda_\omega V_{0N}\right) = 0, \tag{21}$$

$$\sum_{B=N,\Sigma,\Xi}\frac{\partial m^*_B}{\partial m^*_N} M_B \rho_{sB} + \sum_{Y=\Sigma,\Xi}\frac{\partial V_{0Y}}{\partial m^*_N}\rho_{bY} + m^2_\sigma \langle\sigma\rangle \frac{\partial \langle\sigma\rangle}{\partial m^*_N} + m^2_{\sigma^*}\langle\sigma^*\rangle \frac{\partial \langle\sigma^*\rangle}{\partial m^*_N} + \left(\frac{m_\omega}{g^*_{NN\omega}}\right)^2 V^2_{0N}\frac{1}{g^*_{NN\omega}}\frac{\partial g^*_{NN\omega}}{\partial m^*_N} + \left(\frac{m_\phi}{g^*_{\Lambda\Lambda\phi}}\right)^2 \left(V_{0\Lambda} - C^\Lambda_\omega V_{0N}\right)^2 \frac{1}{g^*_{\Lambda\Lambda\phi}}\frac{\partial g^*_{\Lambda\Lambda\phi}}{\partial m^*_N} + \left(\frac{m_\phi}{g^*_{\Lambda\Lambda\phi}}\right)^2 \left(V_{0\Lambda} - C^\Lambda_\omega V_{0N}\right) V_{0N}\frac{1}{g^*_{NN\omega}}\left(\frac{\partial g^*_{\Lambda\Lambda\omega}}{\partial m^*_N} - \frac{g^*_{\Lambda\Lambda\omega}}{g^*_{NN\omega}}\frac{\partial g^*_{NN\omega}}{\partial m^*_N}\right) = 0, \tag{22}$$

$$\sum_{Y=\Lambda,\Sigma,\Xi}\frac{\partial m^*_Y}{\partial m^*_\Lambda} M_Y \rho_{sY} + \sum_{Y=\Sigma,\Xi}\frac{\partial V_{0Y}}{\partial m^*_\Lambda}\rho_{bY} + m^2_{\sigma^*}\langle\sigma^*\rangle \frac{\partial \langle\sigma^*\rangle}{\partial m^*_\Lambda} + \left(\frac{m_\phi}{g^*_{\Lambda\Lambda\phi}}\right)^2 \left(V_{0\Lambda} - C^\Lambda_\omega V_{0N}\right) V_{0N}\frac{1}{g^*_{NN\omega}}\frac{\partial g^*_{\Lambda\Lambda\omega}}{\partial m^*_\Lambda} + \left(\frac{m_\phi}{g^*_{\Lambda\Lambda\phi}}\right)^2 \left(V_{0\Lambda} - C^\Lambda_\omega V_{0N}\right)^2 \frac{1}{g^*_{\Lambda\Lambda\phi}}\frac{\partial g^*_{\Lambda\Lambda\phi}}{\partial m^*_\Lambda} = 0. \tag{23}$$

The calculations of the derivatives by m^*_N and m^*_Λ in Eqs. (22) and (23) are tedious but straightforward tasks and so their explicit expressions are not shown here.

The baryon and scalar densities in Eqs. (20)-(23) are defined by

$$\rho_{bB} = \gamma_B \int_0^\infty \frac{d^3\mathbf{k}}{(2\pi)^3} \left[n_{kB}(T) - \bar{n}_{kB}(T) \right], \tag{24}$$

$$\rho_{sB} = \gamma_B \int_0^\infty \frac{d^3\mathbf{k}}{(2\pi)^3} \frac{M_B^*}{E_{kB}^*} \left[n_{kB}(T) + \bar{n}_{kB}(T) \right], \tag{25}$$

where the Fermi-Dirac distribution functions of each baryon and antibaryon are

$$n_{kB}(T) = \left[1 + \exp\left(\frac{E_{kB}^* - \nu_B}{T} \right) \right]^{-1}, \tag{26}$$

$$\bar{n}_{kB}(T) = \left[1 + \exp\left(\frac{E_{kB}^* + \nu_B}{T} \right) \right]^{-1}. \tag{27}$$

3 Numerical analyses

Because of the chemical equilibrium condition [22]

$$\mu_\Lambda = \mu_\Sigma = \frac{\mu_N + \mu_\Xi}{2}, \tag{28}$$

the chemical potentials of Σ and Ξ are determined by those of N and Λ. Under a definite temperature T, the total baryon density

$$\rho_T = \sum_{B=N,\Lambda,\Sigma,\Xi} \rho_{bB} \tag{29}$$

and the strangeness fraction

$$f_S = \frac{\rho_{b\Lambda} + \rho_{b\Sigma} + 2\rho_{b\Xi}}{\rho_T}, \tag{30}$$

Eqs. (20)-(23), (29) and (30) have to be solved numerically utilizing 6-dimensional Newton-Raphson method so that the effective masses m_N^* and m_Λ^*, the vector potentials V_{0N} and $V_{0\Lambda}$, and the chemical potentials μ_N and μ_Λ are determined selfconsistently.

For the calculations we have to specify the meson-baryon coupling constants. The $g_{NN\sigma}$ and $g_{NN\omega}$ were determined [14] so as to reproduce the nuclear matter saturation properties. Unfortunately, the meson-hyperon coupling constants are not well known at present. In fact, the recent investigations [17-19] of liquid-gas phase transition in SHM employed different coupling constants from each other. Here we follow the prescription of Ref. [22]. First, the $g_{\Lambda\Lambda\omega}$, $g_{\Sigma\Sigma\omega}$ and $g_{\Xi\Xi\omega}$ are fixed by the SU(6) relations:

$$\frac{1}{3} g_{NN\omega} = \frac{1}{2} g_{\Lambda\Lambda\omega} = \frac{1}{2} g_{\Sigma\Sigma\omega} = g_{\Xi\Xi\omega}. \tag{31}$$

On the other hand, the $g_{\Lambda\Lambda\sigma}$, $g_{\Sigma\Sigma\sigma}$ and $g_{\Xi\Xi\sigma}$ are chosen so as to predict reasonable hyperon potentials in saturated nuclear matter at $\rho_{nm} = 0.16\,\mathrm{fm}^{-3}$:

$$U_\Lambda^{(N)}(\rho_{nm}) = -28\,\mathrm{MeV}, \quad U_\Sigma^{(N)}(\rho_{nm}) = 30\,\mathrm{MeV} \quad \text{and} \quad U_\Xi^{(N)}(\rho_{nm}) = -18\ \mathrm{MeV}. \tag{32}$$

The obtained values are

$$\frac{g_{\Lambda\Lambda\sigma}}{g_{NN\sigma}} = 0.604, \quad \frac{g_{\Sigma\Sigma\sigma}}{g_{NN\sigma}} = 0.461 \quad \text{and} \quad \frac{g_{\Xi\Xi\sigma}}{g_{NN\sigma}} = 0.309. \tag{33}$$

The $YY\phi$ coupling constants are also fixed by the SU(6) relations:

$$2\,g_{\Lambda\Lambda\phi} = 2\,g_{\Sigma\Sigma\phi} = g_{\Xi\Xi\phi} = -\frac{2\sqrt{2}}{3}\,g_{NN\omega}. \tag{34}$$

Of course $g_{NN\phi} = 0$. On the other hand, the $\Lambda\Lambda\sigma^*$ and $\Xi\Xi\sigma^*$ coupling constants are determined so as to reproduce the binding energy curves of pure Λ and Ξ matter in the Brueckner-Hartree-Fock calculation [23] using the Nijmegen soft-core potential model NSC97f [24,25]. Although the Nijmegen potential can reproduce the recent data of ${}^{\ 6}_{\Lambda\Lambda}\mathrm{He}$ [26] within the three-body Faddeev calculation [27], it predicts a rather deep saturation of pure Σ matter [23]. If the $\Sigma\Sigma\sigma^*$ coupling constant is determined in the same way as $\Lambda\Lambda\sigma^*$ and $\Xi\Xi\sigma^*$, it becomes much stronger than the value derived from SU(6) symmetry. The strong $g_{\Sigma\Sigma\sigma^*}$ predicts the first-order phase transition [21,22,28] from the SHM consisting of $N + \Lambda + \Xi$ to the SHM with dominant abundance of Σ above $f_S = 1.0$. It is however not clear whether such a phase transition really occurs. Therefore, only for $g_{\Sigma\Sigma\sigma^*}$ we do not follow the prescription of Ref. [22] and take the same $\Sigma\Sigma\sigma^*$ and $\Lambda\Lambda\sigma^*$ coupling constants according to the SU(6) symmetry. Consequently, we have

$$\frac{g_{\Lambda\Lambda\sigma^*}}{g_{NN\sigma}} = \frac{g_{\Sigma\Sigma\sigma^*}}{g_{NN\sigma}} = 0.52 \quad \text{and} \quad \frac{g_{\Xi\Xi\sigma^*}}{g_{NN\sigma}} = 1.28. \tag{35}$$

Of course $g_{NN\sigma^*} = 0$.

Figures 1-4 calculate the pressure-density isotherms for $f_S = 0.5$, 1.0, 1.5 and 2.0, respectively. They behave like van der Waals equation-of-state and show the liquid-gas phase transitions. The critical temperatures T_C and the pressures P_C and densities ρ_C at the inflection points are summarized in Table 1. Here it is however noted that in the above formulation of the SHM the pure Ξ matter ($f_S = 2$) cannot be realized physically at finite temperature because there are a little fractions of other baryons due to the tails in the Fermi-Dirac distributions. Nevertheless, we can calculate the virtual pure Ξ matter if the densities of the other baryons in Eqs. (20)-(23) are set to zero from the first. In this case there is only the chemical potential of Ξ and so Eqs. (28) and (30) are lost. Equations (20)-(23) and (29) are solved numerically utilizing 5-dimensional Newton-Raphson method so that the effective masses m_N^* and m_Λ^*, the vector potentials V_{0N} and $V_{0\Lambda}$, and the chemical potential μ_Ξ are determined selfconsistently.

The dependence of T_C and ρ_C on the strangeness fraction is shown in Fig. 5. The critical temperature decreases in $f_S < 0.5$ but increases in $f_S > 0.5$. Above $f_S = 1$ it becomes larger than 16.4 MeV for normal ($f_S = 0$) nuclear matter. The result is essentially due to the NSC97 potential [23], by which the pure Ξ matter has deeper saturation at higher density than the normal nuclear matter while the pure Λ matter has no saturation. In the SHM with low strangeness fraction, Λ is more abundant than Ξ and so the shallower binding due to Λ matter leads to lower critical temperature of the SHM than the normal nuclear matter. On the contrary, in the SHM with high strangeness fraction, Ξ is dominantly abundant over the other baryons and so the deeper binding due to Ξ matter leads to higher critical temperature of the SHM than the normal nuclear matter. (In the present calculation there is little Σ fraction to be neglected.) In contrast to the behavior of T_C, the density ρ_C increases as the strangeness fraction increases up to $f_S = 1.5$ and then turns to decrease. This turning is reflected in the moderate increase of T_C at $f_S > 1.5$ although the rapid increase is recovered near $f_S = 2$.

Because there are two conserved quantities, the baryon number and strangeness, or the two independent chemical potentials, the SHM is usually regarded [17-19] as two-component system. The situation is the same as the asymmetric nuclear matter [29], in which the proton and neutron are independent components because their chemical potentials are different from each other due to the isovector-meson mean-fields. It is known [30] that the phase transition in the two-component system is of second order in Ehrenfest's definition. This is however inconsistent with the analyses [6,11] of multifragmentation reactions, in which the liquid-gas phase transition of nuclear matter is treated as the first-order one.

For the comparison with the experimental analyses, in the previous work [13] we treated the liquid-gas phase transition in asymmetric nuclear matter as the first-order one. Because the main purpose of the present work is to confirm the universality of the critical phenomena in hadronic matter, we also treat the liquid-gas phase transition in SHM as the first-order one. In other words we consider the equilibrium between the Gibbs energy per particle $\tilde{G} = (\sum \mu_B \rho_{bB})/\rho_T$ rather than each chemical potential in the equilibrated liquid and gas phases. The phase coexistence curve is therefore determined by the Maxwell construction. The solid, dashed, dotted and dotted-dashed curves in Fig. 6 show the results in temperature-density plain for the strangeness fraction $f_S = 0.5$, 1.0, 1.5 and 2.0, respectively. It is seen that the coexistence regions extend over much wider density ranges than those [12,13] in normal nuclear matter. This is also because that the SHM with $f_S \geq 1.0$ has dominant Ξ fraction and the pure Ξ matter by the NSC97 potential has a saturation point at much higher density than the normal nuclear matter. We also find that the coexistence region for $f_S = 1.5$ is wider than that for $f_S = 2.0$ in accordance with the behavior of ρ_C in Fig. 5.

As seen above, the strangeness has large effects on the liquid-gas phase transitions in hadronic matter. Does the strangeness also affect the critical phenomena in SHM? The

upper panels in Figs. 7-10 show the differences between the densities of equilibrated liquid and gas phases on the phase coexistence curves in Fig. 6 as functions of temperature in log scale. The lower panels show the inverses of incompressibility κ on the liquid branches of the coexistence curves:

$$\frac{1}{\kappa} \propto \frac{\rho_B}{P_C}\frac{\partial P}{\partial \rho_B} \propto \left(1 - \frac{T}{T_C}\right)^{\gamma}. \tag{36}$$

The circles in Fig. 7 are calculated on the solid curve in Fig. 6 at $T = 5.0$, $6.0 \cdots 14.0$, $14.2 \cdots 14.8$ MeV. The circles in Figs. 8, 9 and 10 are calculated on the dashed curve at $T = 6.0$, $7.0 \cdots 16.0$, $16.2 \cdots 16.8$ MeV, on the dotted curve at $T = 8.0$, $9.0 \cdots 18.0$, 18.5, 19.0, $19.2 \cdots 20.0$ MeV and on the dotted-dashed curve at $T = 8.0$, $9.0 \cdots 21.0$, 21.5, 22.0, 22.2 and 22.4 MeV, respectively.

The calculated values satisfy the so-called power law. In the upper panels of figures they lie on the red and blue lines in the near region to and the far region from the critical point respectively, while in the lower panels they lie on the single blue lines over the whole region of temperature. The inclinations of the lines in the upper and lower panels are nothing but the critical exponents β and γ, respectively. The obtained value of β from the red lines is 0.48 and the value of γ is 1.22 regardless of the strangeness fraction. They agree with the corresponding values from nonstrange isospin-symmetric [12] and asymmetric [13] nuclear matter. It is however noted [11] that in heavy-ion reactions the limit of Coulomb instability prevents the nuclear system from reaching the critical point and so the critical exponents have been derived [10] in the far region from the critical point. According to this fact, Figs. 7-10 predict $\beta = 0.31$, 0.34, 0.32 and 0.31 respectively from the blue lines rather than $\beta = 0.48$ from the red lines. Although the values slightly fluctuate with increasing strangeness fraction, they almost agree with each other and with those derived from multifragmentation reactions [6,8-10] and the universal value of the liquid-gas phase transition. We have therefore confirmed the universality of the critical phenomena in liquid-gas phase transition of hadronic system.

4 Summary

We have studied the thermodynamics of strange hadronic matter in the EZM model including the (hidden) strange mesons. The equation-of-state behaves like van der Waals one and so clearly shows the liquid-gas phase transition. For the hyperon-hyperon interactions, we implement the Nijmegen soft-core potential model NSC97f by adjusting the strange meson coupling constants. Because this potential predicts no saturation of pure Λ matter but a deep saturation of pure Ξ matter, the SHM with relatively large Λ fraction has lower critical temperature than the normal nuclear matter while the SHM with dominant Ξ fraction has higher critical temperature.

For calculating the liquid-gas phase coexistence curve in the pressure-density plain,

we treat the phase transition as the first-order one and employ the Maxwell construction. This prescription is consistent to the experimental analyses of recent multifragmentation reactions. Then the critical exponents β and γ are derived for several strangeness fractions. The obtained values from the near region to the critical point are independent of the strangeness fraction. Although the values of β in the far region from the critical point slightly vary with the strangeness, our calculated exponents almost agree with their universal values and the empirical values derived from multifragmentation reactions. Consequently, the universality of the critical phenomena in the liquid-gas phase transition of hadronic matter has been confirmed.

References

[1] J. Richert and P. Wagner, Phys. Rep. **350** (2001) 1 [arXiv:nucl-th/0009023]

[2] S.D. Gupta, A.Z. Mekjian and M.B. Tsang, *Advances in Nuclear Physics*, Vol. **26** (Kluwer Academic, 2001) [arXiv:nucl-th/0009033].

[3] J.B. Natowitz *et al.*, Phys. Rev. **C65** (2002) 034618 [arXiv:nucl-ex/0106016].

[4] M. D'Agostino *et al.*, Phys. Lett. **B473** (2000) 219 [arXiv:nucl-ex/9906004]; B. Borderie *et al.*, Nucl. Phys. **A734** (2004) 495 [arxiv:nucl-ex/0311016].

[5] V.A. Karnaukhov *et al.*, Phys. Rev. **C67** (2003) 011601 [arXiv:nucl-ex/0302006].

[6] J.B. Elliott *et al.*, Phys. Rev. **C67** (2003) 024609 [arXiv:nucl-ex/0205004].

[7] J.B. Natowitz *et al.*, Phys. Rev. Lett. **89** (2002) 212701 [arXiv:nucl-ex/0204015].

[8] B.K. Srivastava *et al.*, Phys. Rev. **C65** (2002) 054617 [arXiv:nucl-ex/0202023].

[9] D. Kudzia, B. Wilczyńska and H. Wilczyński, Phys. Rev. **C68** (2003) 054903 [arXiv:nucl-ex/0207017].

[10] Y.G. Ma *et al.*, Phys. Rev. **C71** (2005) 054606 [arXiv:nucl-ex/0410018].

[11] J.B. Natowitz *et al.*, arXiv:nucl-ex/0206010.

[12] K. Miyazaki, Mathematical Physics Preprint Archive (mp_arc) 05-261.

[13] K. Miyazaki, Mathematical Physics Preprint Archive (mp_arc) 05-325.

[14] K. Miyazaki, Mathematical Physics Preprint Archive (mp_arc) 05-178

[15] K. Miyazaki, Mathematical Physics Preprint Archive (mp_arc) 05-190.

[16] B.D. Serot and J.D. Walecka, *Advances in Nuclear Physics*, Vol. **16** (Plenum, New York, 1986).

[17] L. Yang, W.L. Qian, R.K. Su and H.Q. Song, Phys. Rev. **C70** (2004) 045207 [arXiv:nucl-th/0311017];

[18] W.L. Qian, R.K. Su and H.Q. Song, J. Phys. **G30** (2004) 1893 [arXiv:nucl-th/0409063].

[19] P. Wang. D.B. Leinweber, A.W. Thomas and A.G. Williams, Phys. Rev. **C70** (2004) 055204 [arXiv:nucl-th/0407056].

[20] J. Schaffner, C.B. Dover, A. Gal, C. Greiner and H. Stőker, Phys. Rev. Lett. **71** (1993) 1328.

[21] K. Miyazaki, Mathematical Physics Preprint Archive (mp_arc) 05-216.

[22] J. Schaffner-Bielich and A. Gal, Phys. Rev. **C62** (2000) 034311 [arXiv:nucl-th/0005060].

[23] V.G.J. Stoks and T.-S.H. Lee, Phys. Rev. **C60** (1999) 024006 [arXiv:nucl-th/9901030].

[24] V.G.J. Stoks and Th.A. Rijken, Phys. Rev. **C59** (1999) 3009 [arXiv:nucl-th/9901028].

[25] Th.A. Rijken, V.G.J. Stoks and Y. Yamamoto, Phys. Rev. **C59** (1999) 21 [arXiv:nucl-th/9807082].

[26] H. Takahashi *et al.*, Phys. Rev. Lett. **87** (2001) 212502.

[27] I.N. Filikhin and A. Gal, Phys. Rev. **C65** (2002) 041001(R); Nucl. Phys. **A707** (2002) 491 [arXiv:nucl-th/0203036]; I.N. Filikhin, A. Gal and V.M. Suslov, Phys. Rev. **C68** (2003) 024002 [arXiv:nucl-th/0303028]; Nucl. Phys. **A743** (2004) 194 [arXiv:nucl-th/0406049];

[28] I. Zakout, H.R. Jaqaman, H. Stőker and W. Greiner, J. Phys. **G27** (2001) 1939 [arXiv:nucl-th/005005].

[29] H. Műller and B. D. Serot, Phys. Rev. **C52** (1995) 2072 [arXiv:nucl-th/9505013].

[30] L. Yang, S.Y. Yin, W.L. Qian, and R.K. Su, arXiv:nucl-th/0506060.

Table 1: The critical temperatures and the pressures and densities at inflection points in the pressure-density isotherm for several strangeness fractions.

	$f_S = 0.0$	$f_S = 0.5$	$f_S = 1.0$	$f_S = 1.5$	$f_S = 2.0$
$T_C\,(\mathrm{MeV})$	16.360	14.972	16.937	20.110	22.539
$P_C\,\left(\mathrm{MeV/fm^3}\right)$	0.3078	0.4313	0.8072	1.221	1.032
$\rho_C\,(\mathrm{fm^{-3}})$	0.059	0.086	0.134	0.173	0.142

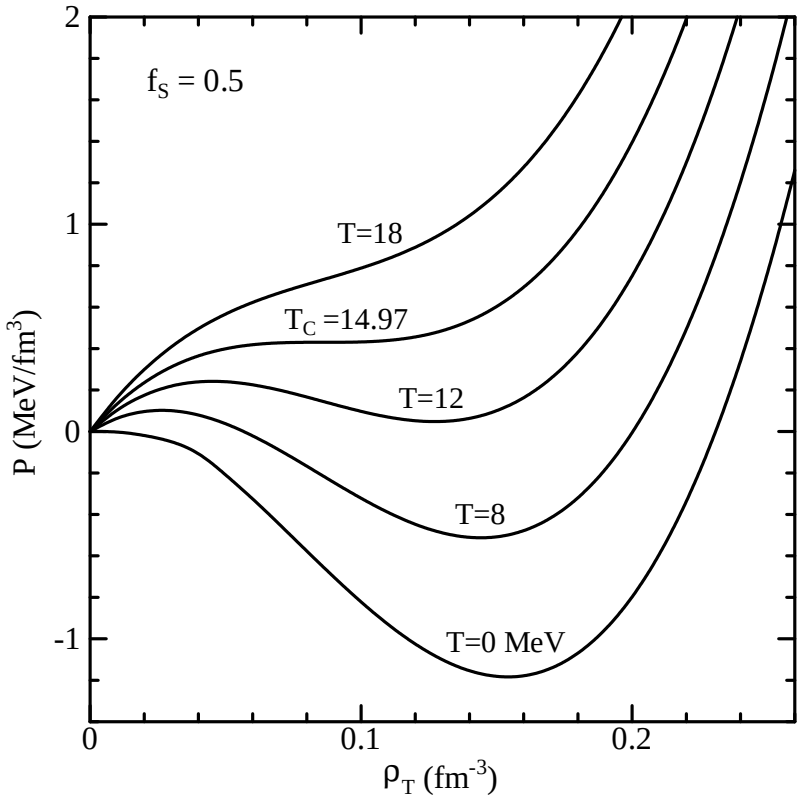

Figure 1: The pressure-density isotherms of SHM for the strangeness fraction $f_S = 0.5$.

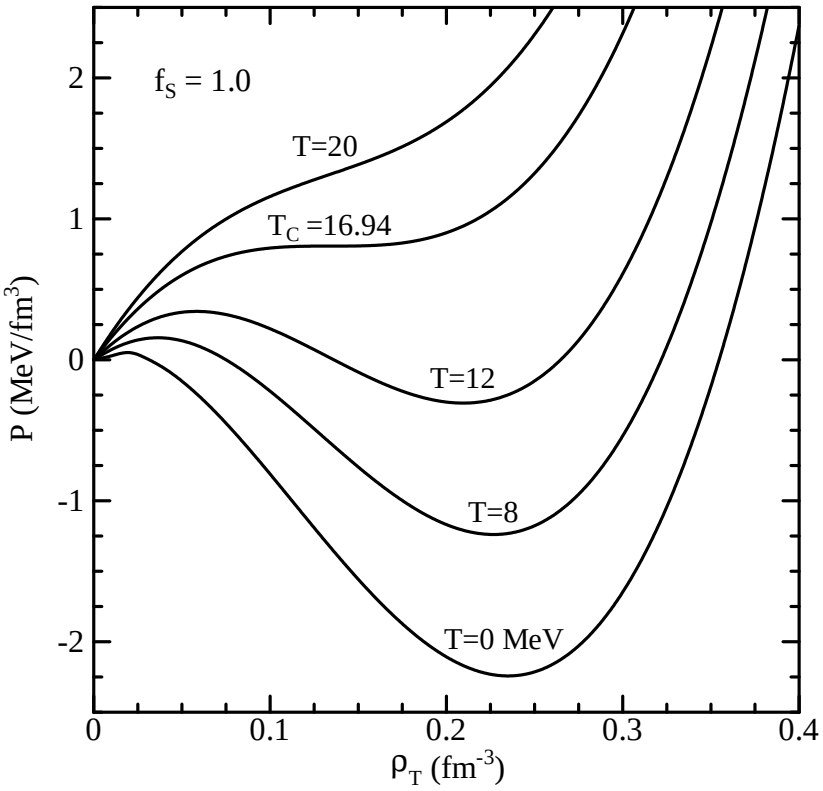

Figure 2: The same as Fig. 1 but for $f_S = 1.0$.

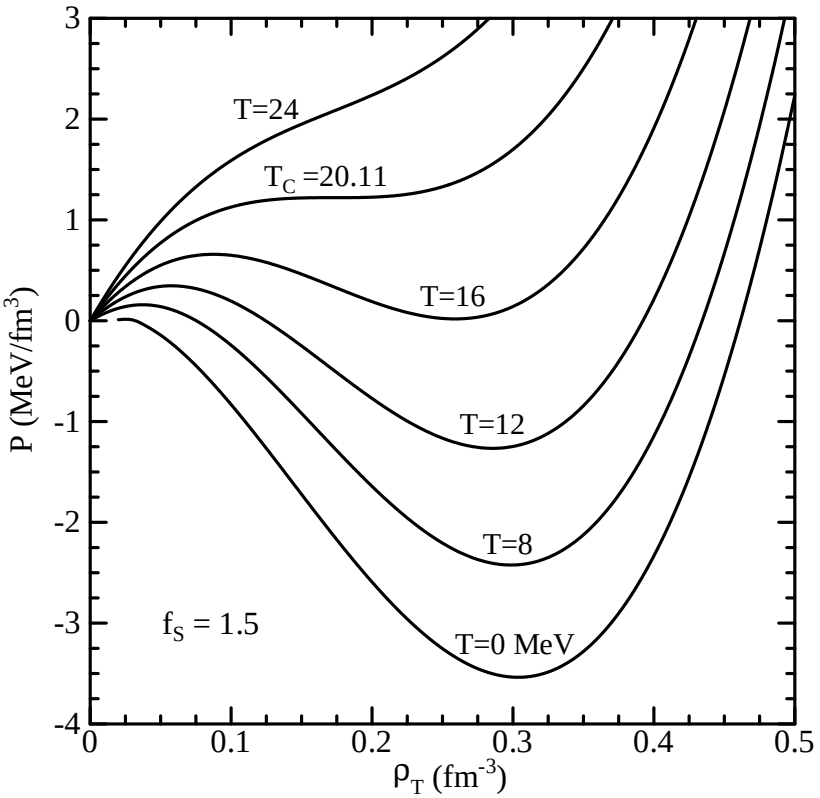

Figure 3: The same as Fig. 1 but for $f_S = 1.5$.

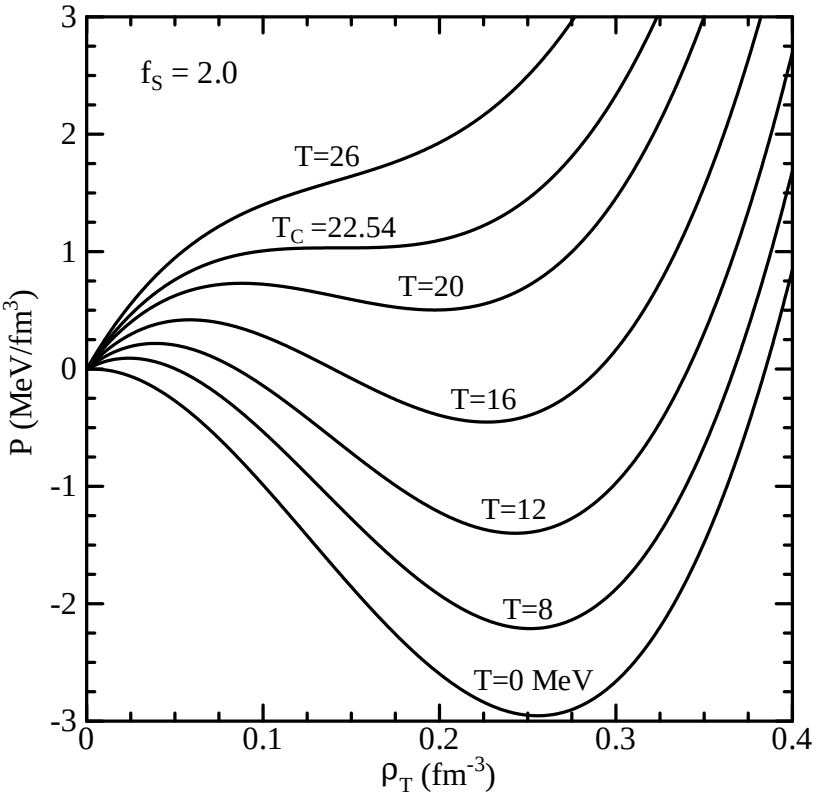

Figure 4: The same as Fig.1 but for $f_S = 2.0$.

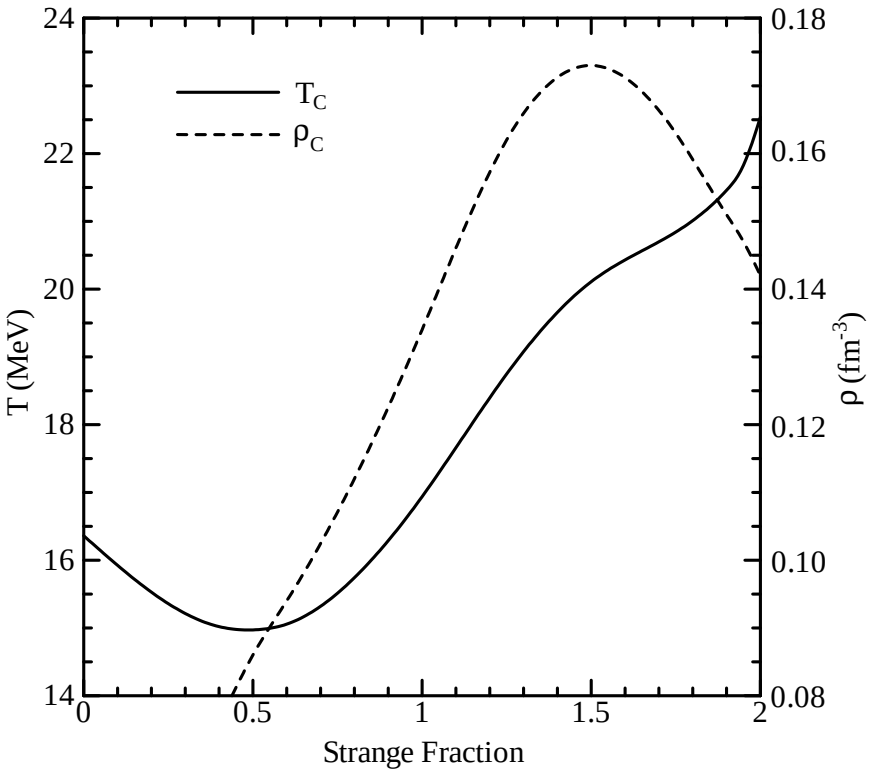

Figure 5: The dependence of the critical temperature T_C and density ρ_C on the strangeness fraction.

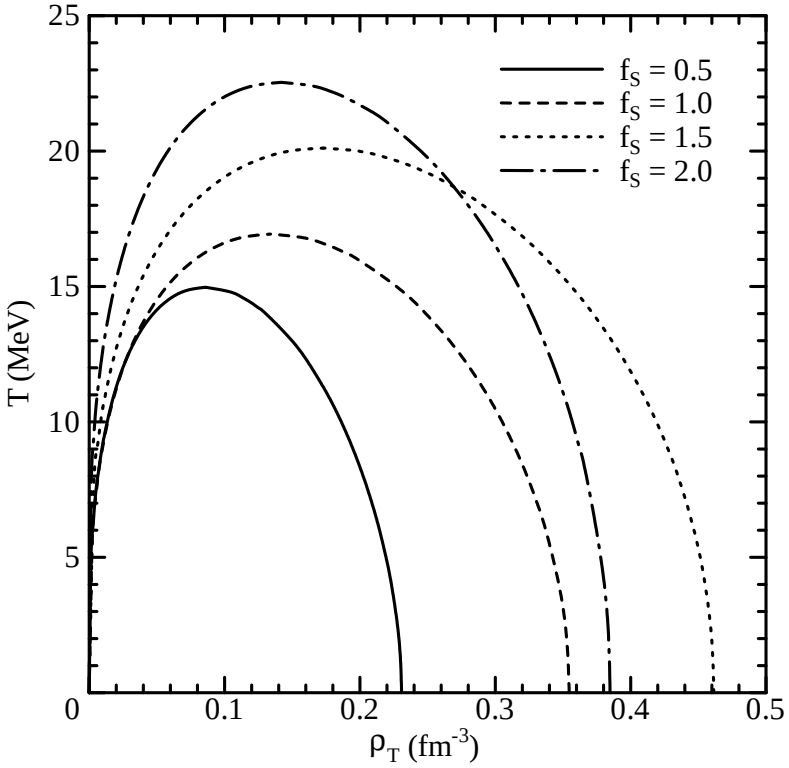

Figure 6: The liquid-gas phase coexistence curves in temperature-density plain. The solid, dashed, dotted and dotted-dashed curves are for the strangeness fraction $f_S = 0.5$, 1.0, 1.5 and 2.0, respectively.

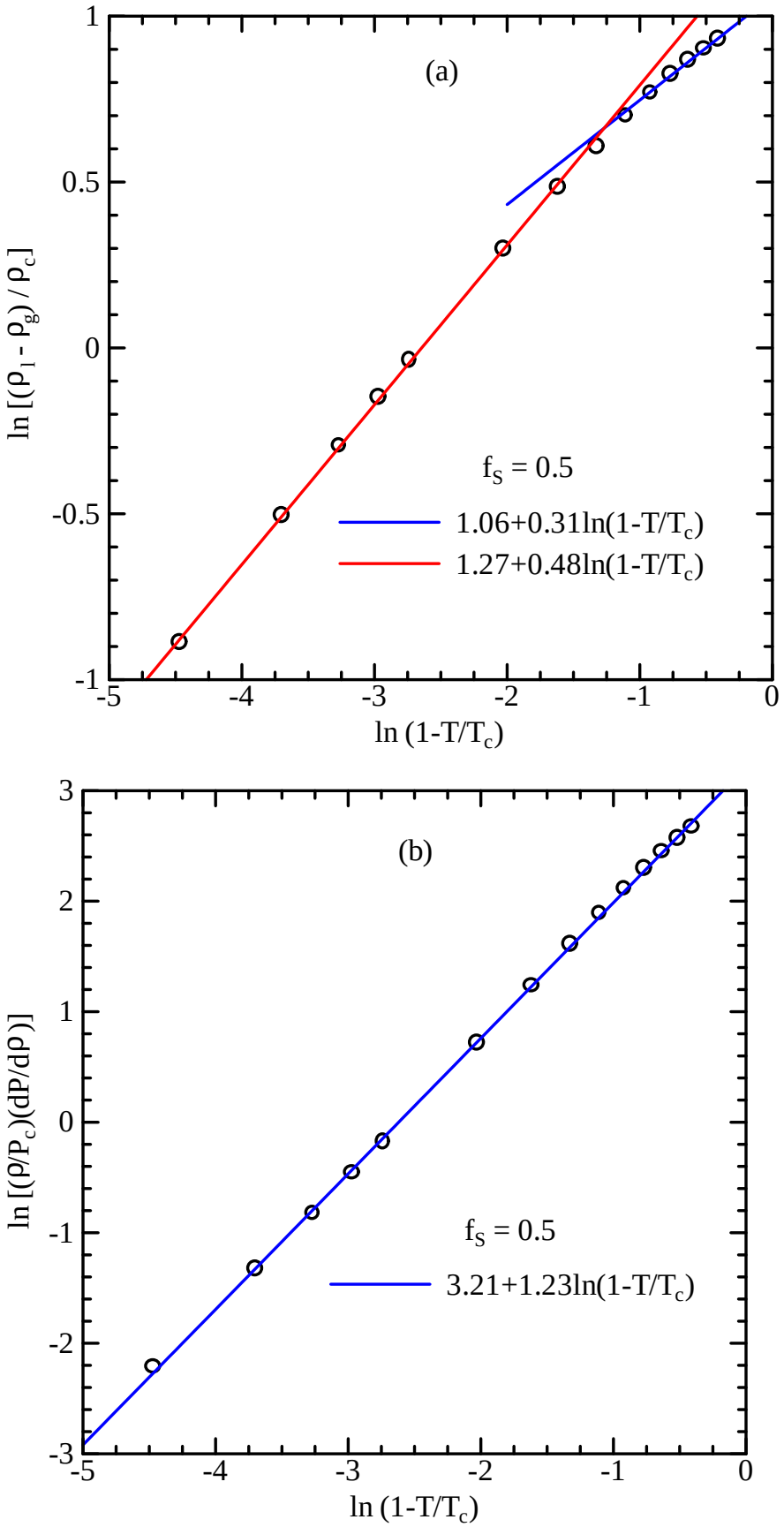

Figure 7: (a) The difference between the densities of the equilibrated liquid and gas phases and (b) the inverse of compressibility of nuclear liquid as functions of temperature in log scale calculated on the solid curve in Fig. 6.

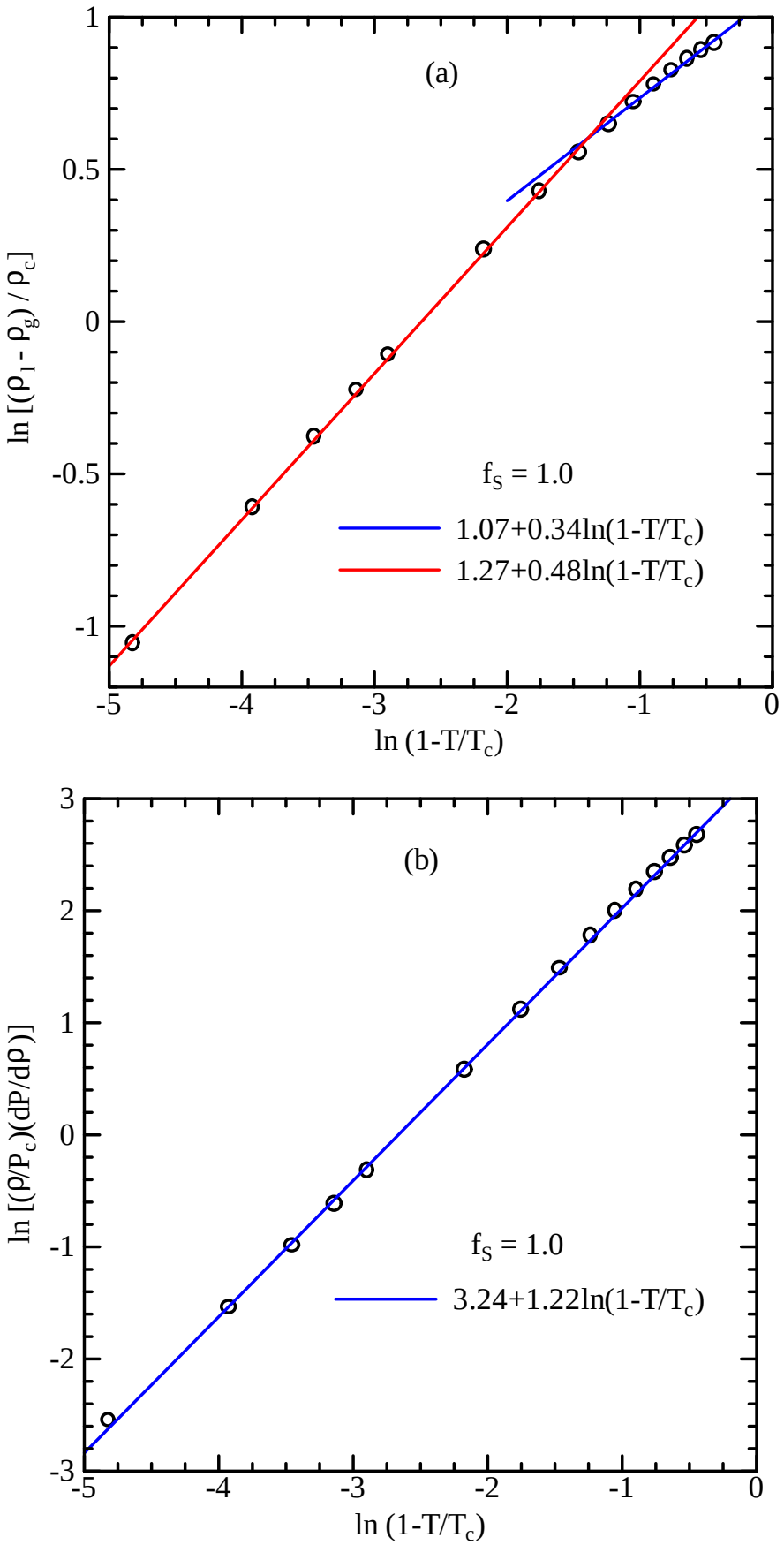

Figure 8: The same as Fig. 7 but for the strangeness fraction $f_S = 1.0$.

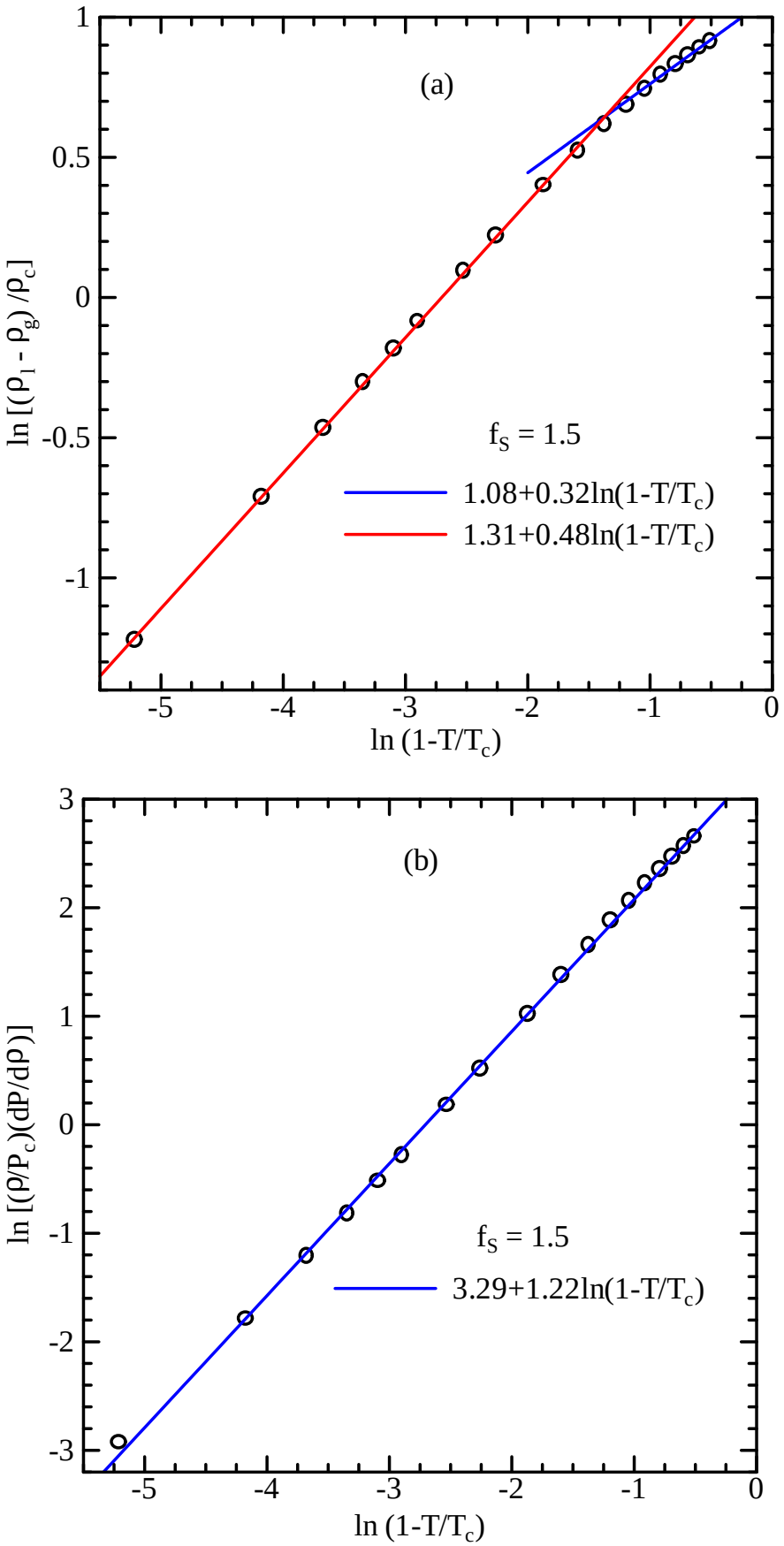

Figure 9: The same as Fig. 7 but for the strangeness fraction $f_S = 1.5$.

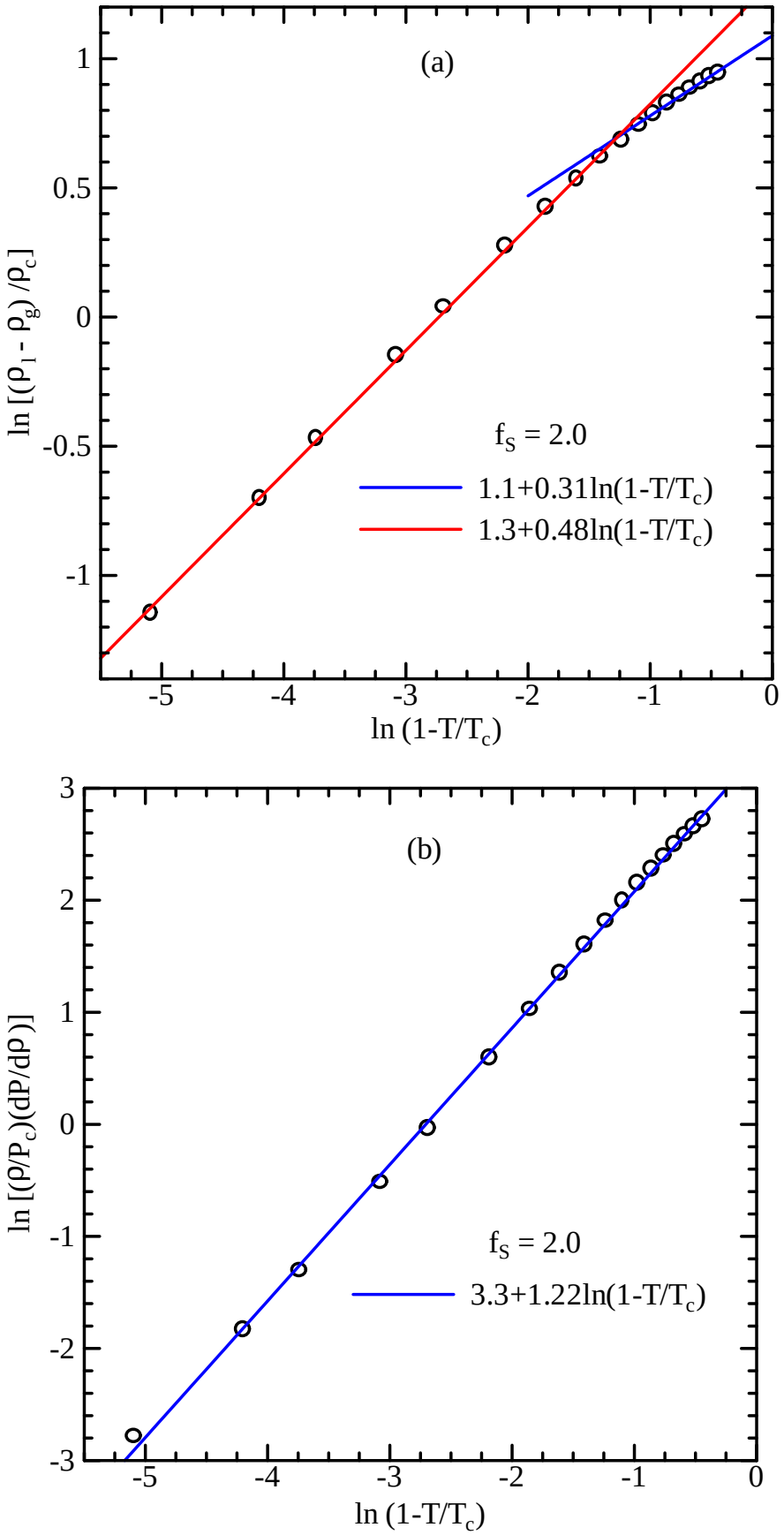

Figure 10: The same as Fig. 7 but for the strangeness fraction $f_S = 2.0$.